Lightweight Wheel Hub Design for New Energy Vehicles Based on ANSYS Workbench

Yuyang Zhao *

Sino-European School of Technology, Shanghai University, Baoshan District, Shanghai, 200444, China

* Corresponding Author Email: Yuyang Zhao: 2726346738@qq.com

Abstract. Driven by the national "Dual Credit" policy, the automotive industry is advancing towards electrification and lightweighting. In this context, the lightweight design of new energy vehicle hubs plays a crucial role in improving driving range, reducing energy consumption, and enhancing maneuverability. This paper uses claw and petal shapes as design elements to create a 3D model of the hub in Creo Parametric. By referring to the parameters of a specific SUV, 6061-T6 aluminum alloy is chosen as the material. Finite element methods are employed in ANSYS Workbench to simulate radial loads, bending loads, and modal analysis. Through continuous topology optimization, a hub with a mass of 8.9 kg is designed, meeting lightweight standards while satisfying various performance requirements. This design has significant reference value for actual production.

Keywords: Wheel hub, Lightweighting, Finite Element Method.

1. Introduction

The automotive industry is closely linked to energy, environment, and climate change. The massive consumption of fossil fuels and the emission of greenhouse gases and pollutants by traditional fuel vehicles have made them a focal point in global efforts to address climate change and build a clean, low-carbon world, with the development of new energy vehicles being seen as a crucial solution to the energy crisis and environmental protection [1].

Although new energy vehicles are developing rapidly and are increasingly favored by consumers, driving range has always been a "pain point" that affects consumer purchase decisions. Given that battery technology has reached a bottleneck, reducing vehicle body mass is an effective way to improve the cruising range of new energy vehicles. Additionally, a lighter vehicle can reduce the time required for acceleration, lower the operating load on the engine, and decrease the probability of failures [2], which significantly enhances the car's performance.

The lightweighting of a new energy vehicle as a whole is the sum of the lightweighting of its individual components, such as using an aluminum alloy frame for the car body and magnesium alloy for the instrument panel and seat frames. The wheel hub is an important part of the vehicle's drive assembly, which transmits the driving force from the drive axle to the wheel through the rim [3]. The wheel hub's varied appearance and structure offer a vast space for innovative design. The goal of this paper is to design a lightweight wheel hub that can be applied to actual production, and to give it an innovative appearance.

2. Wheel hub model

2.1. Wheel hub structure

Figure 1. A three-dimensional schematic diagram of the wheel hub

As shown in Figure 1, the wheel hub structure is mainly divided into the rim, spokes, and mounting disc. The rim section is further divided into the wheel flange and bead seat. The mounting disc is distributed with bolt holes and a center hole. The rim is the outer circular metal structure of the wheel that directly contacts and supports the tire. The offset is the distance from the mounting surface of the wheel hub (the plane that contacts the vehicle's axle head) to the centerline of the wheel hub (the midpoint of the rim width). The bead seat is the specially designed area on the rim that supports the tire bead, typically consisting of two slightly inclined shoulders. The wheel flange is the outermost edge of the rim, extending upward from the bead seat to form a "protrusion." The spokes are the parts connecting the rim to the central disc of the hub, radiating outward from the center.

2.2. Wheel hub model

The wheel hub design adopts a biomimetic concept inspired by eagle claws and employs a multi-branch configuration to alleviate stress concentration. Claw-like structures are commonly found in both natural organisms and engineering applications, such as animal claws (Figure 2) and industrial mechanical grippers (Figure 3). This biomimetic morphology establishes continuous load-bearing paths in multiple directions, thereby exhibiting superior resistance to complex loading conditions (e.g., braking torque). Compared with conventional straight-spoke designs, it provides improved torsional rigidity. Moreover, in the event of partial spoke failure, the remaining claw-like branches can still sustain structural support, thereby enhancing redundancy and fault tolerance.

Figure 2. Eagle's talons

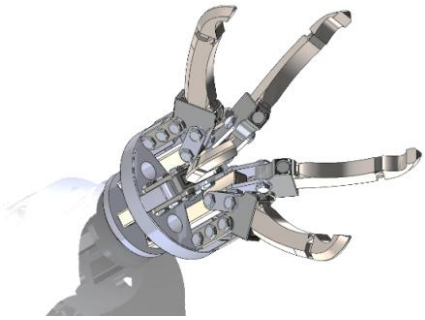

Figure 3. Industrial mechanical claw

Building upon the claw-shaped configuration, a petal-inspired morphology is integrated to further reinforce the structure while enhancing its aesthetic appeal. In addition, hollowing treatment is applied to the overall geometry with the aim of reducing material usage. The parameters of the wheel hub are summarized in Table 1, and the corresponding model is illustrated in Figure 4.

Table 1. Wheel hub parameters

Nominal Diameter	Rim Width	Rim Type	Wheel Offset	PCD
18 inches	8 inches	J	45	5×112

Figure 4. A three-dimensional model of a wheel hub

3. Finite Element Model

3.1. Finite Element Method

The finite element method (FEM) is an advanced mathematical analysis technique. Its fundamental idea is to treat a complex structure or object as an assembly of a finite number of discrete elements connected only at nodes. This approach, which first "divides the whole into parts" and then "reassembles the parts into a whole" while transforming unknowns into knowns, has universal significance and represents one of the fundamental methods in scientific research [4].

FEM has developed rapidly and has been widely applied. Prem J et al [5] employed FEM to simulate wheel hubs, revealing performance differences among steel, aluminum, and magnesium alloy hubs, and identifying the locations of maximum stress. Zhou D. [6] used FEM for the lightweight design of aluminum steering knuckles, providing scientific and technical support for lightweight automotive suspension systems. Ferran et al. [7] investigated the influence of spoke thickness on wheel hub and vehicle mass using FEM. Theja M. S. et al. [8] conducted static and fatigue FEM analyses on aluminum wheel hubs to determine their safe load limits. Adigio E. M. et al. [9] analyzed radial loads on wheel hubs at specified rotational speeds using ANSYS, summarizing fatigue behavior under such operating conditions.

3.2. Mesh Generation

ANSYS offers multiple mesh types, with tetrahedral and hexahedral elements being the most commonly employed. While hexahedral elements typically provide higher computational accuracy, they are less suitable for complex geometries [10]. Considering that wheel hubs feature numerous curved surfaces, such as spokes and bolt holes, tetrahedral elements were selected for meshing. The wheel hub model was imported into ANSYS, and a mesh size of 8 mm was applied. The resulting finite element model, shown in Figure 5, consists of 284,766 elements and 477,152 nodes, ensuring an appropriate balance between computational accuracy and efficiency.

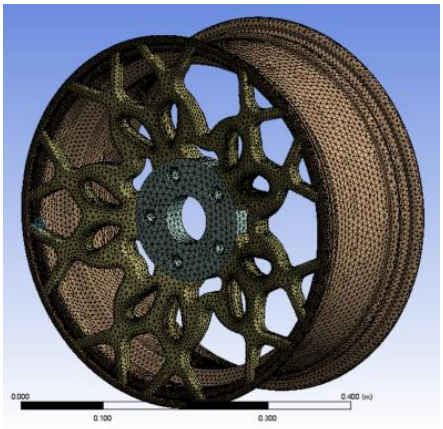

Figure 5. Finite Element Model of the Wheel Hub

3.3. Definition of Material Properties

Aluminum alloys are characterized by low density, excellent wear resistance, high fracture toughness, and high strength, along with good plasticity, making them suitable for automotive component manufacturing and contributing to vehicle lightweighting [11]. Among them, 6061-T6 is a widely used aluminum alloy, primarily alloyed with magnesium and silicon, and can be strengthened through heat treatment. The T6 temper is one of the most commonly applied strengthening states within the 6061 series. 6061-T6 aluminum alloy exhibits high strength, low density (approximately one-third that of steel), as well as good corrosion resistance and toughness, making it extensively used in aerospace, automotive, and marine applications. The material properties are summarized in Table 2:

Table 2. Properties of 6061-T6 Aluminum Alloy

Materials	Density (g/cm^3)	Poisson's ratio	Yield strength (MPa)	Elastic modulus (GPa)
6061-T6	2.7	0.33	276	60

4. Simulation And Analysis

4.1. Overall Vehicle Characteristics

During the simulation analysis, a specific vehicle model was used as a reference to calculate the radial and bending loads acting on the wheel hub. The detailed parameters of the reference vehicle are listed in Table 3:

Table 3. Reference Vehicle Parameters

Vehicle Mass (kg)	Gross Vehicle Weight (kg)	Tire Specifications
2030	2420	235/60 R18

4.2. Radial Load Analysis

4.2.1. Loads and Boundary Conditions

During straight-line driving, the wheels are subjected to repeated vertical loads, such as the vehicle's self-weight and road impacts. Therefore, fatigue analysis under radial loads is necessary to assess whether the wheel hub may fail within the specified number of load cycles. The test method for radial loads is based on the national standard GB/T 5334-2021, "Requirements and Test Methods for Bending and Radial Fatigue Performance of Passenger Car Wheels," with appropriate adjustments made to reflect actual operating conditions.

According to the requirements for determining wheel radial loads specified in GB/T 5334-2021, "Requirements and Test Methods for Bending and Radial Fatigue Performance of Passenger Car Wheels," the calculation formula for the wheel hub radial load is as follows:

$$F_r = F_v \cdot K \tag{1}$$

Where:

F_v—— The maximum vertical static load of the wheel specified by the vehicle or wheel manufacturer, or the rated load of the wheel.

K——Strengthening factor, taken as 2 (see Table 4).

Table 4. Correlation Coefficient of Radial Load

Material	Strengthening Factor K	Minimum Number of Cycles
Steel	2.25	600000
Aluminum Alloy	2	1150000

The maximum load acting on the wheel hub [12] can be expressed as follows:

$$F_{max} = \frac{W_1 \times n_s}{3} + \frac{G}{6} \quad (2)$$

Were,

W_1—— Curb Weight.

n_s—— Load Influence Factor, generally taken as 1.2.

G——Fully Loaded Vehicle Weight.

Based on the parameters of the reference vehicle, the curb weight of the vehicle is 2,030 kg, and the load under fully loaded conditions is $G = (2420 - 2030) \times 9.8 = 3822N$. Therefore, the radial load acting on the wheel hub was calculated to be 17279.2 N.

In addition, the wheel hub is subjected to tire inflation pressure. For the reference tire, the recommended pressure ranges from 2.5 to 2.7 bar. According to Table 5, the test inflation pressure was set at 4.5 bar.

Table 5. Test Inflation Pressure

Tire Inflation Pressure under Service Load (kPa)	Test Inflation Pressure (kPa)
<=160	280
161-280	450
281-450	550
>=450	>= 1.2 times the operating pressure

Since the wheel hub does not directly contact the ground, a gravitational force was applied, with an acceleration due to gravity of 9.8 m/s². Fixed support constraints were imposed on the inner surfaces of the five bolt holes of the wheel hub, and all loads were applied as shown in Figure 6.

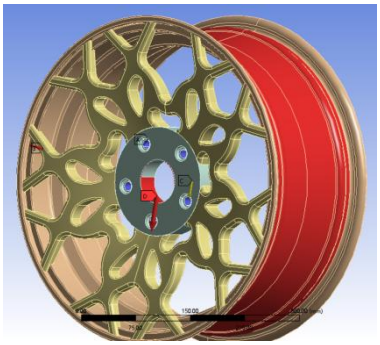

Figure 6. Diagram of Constraints and Loads

4.2.2. Results of Radial Fatigue Analysis

A finite element simulation was conducted to analyze the radial fatigue test of the wheel hub. The results yielded the equivalent stress contour, total deformation contour, fatigue life contour, and safety factor contour of the wheel hub, as shown in Figures 7–9.

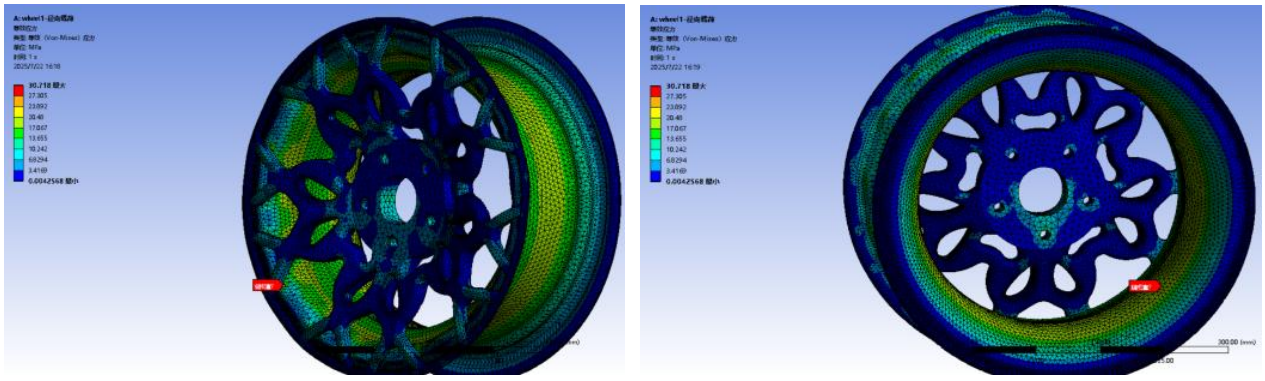

(a) Equivalent Stress Contour (Front View) (b) Equivalent Stress Contour (Rear View)

Figure 7. Stress cloud chart of bending fatigue analysis

Figure 7 shows the equivalent stress contours on the front and rear surfaces of the wheel hub under radial fatigue analysis. The ANSYS simulation indicates that the maximum stress on the wheel hub under radial loading is approximately 30 MPa, which is well below the yield strength of 6061-T6 aluminum alloy (276 MPa), meeting the design requirements. The maximum stress occurs at the contact region between the rim and the spokes on the rear surface of the wheel hub, which is consistent with the stress distribution observed under actual operating conditions.

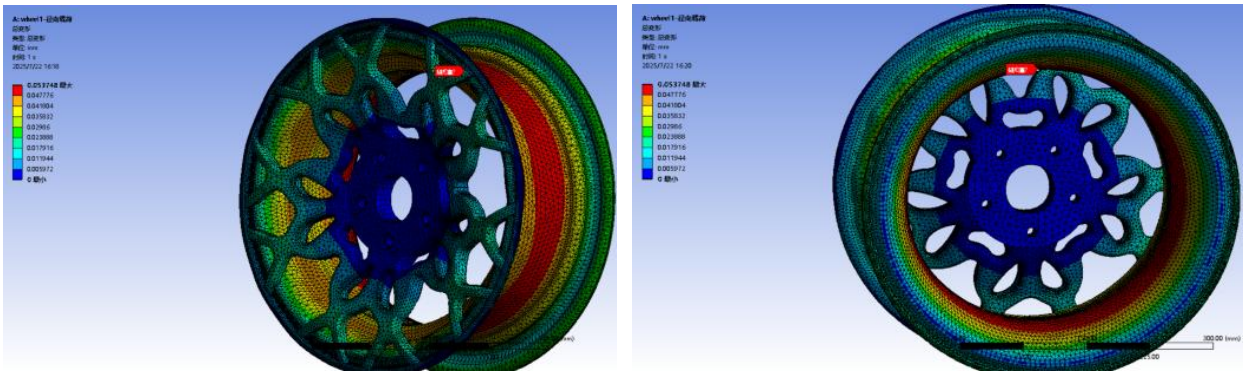

(a) Total Deformation Contour (Front View) (b) Total Deformation Contour (Rear View)

Figure 8. Total Deformation Contour Plot of Radial Fatigue Analysis

Figure 8 shows the total deformation contours on the front and rear surfaces of the wheel hub under radial fatigue analysis. The ANSYS simulation indicates that the maximum deformation under radial loading is approximately 0.05 mm, which is within acceptable limits. The maximum deformation occurs on the rim, and the results meet the design requirements.

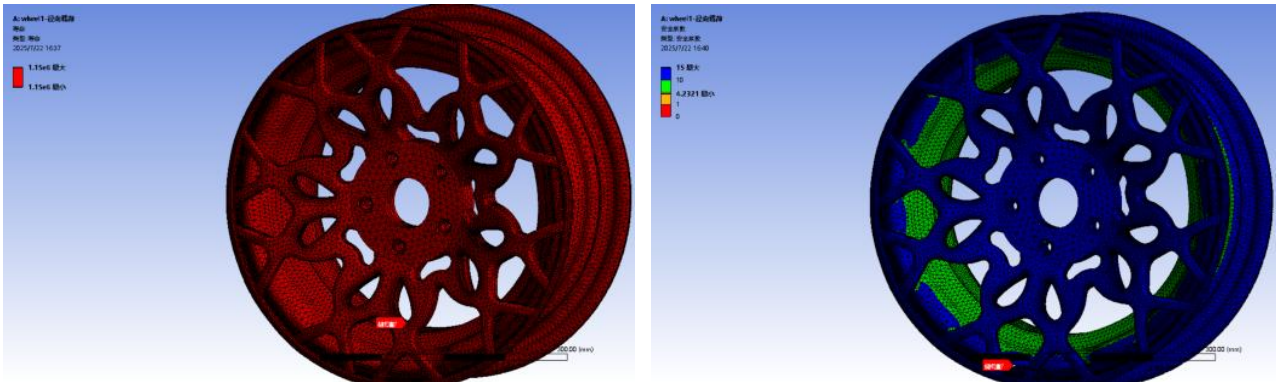

(a) Fatigue Life Contour (b) Safety Factor Contour

Figure 9. Radial fatigue analysis contour plot

Figure 9 presents the fatigue life and safety factor contours under radial loading. Based on Table 3, the cycle number was set to 1,150,000, and an appropriate S-N curve for 6061-T6 aluminum alloy was applied in the engineering data source. The ANSYS results show that the wheel hub structure fully meets the required fatigue life under radial loading. The minimum safety factor is approximately 4.2, located at the junction between the rim and the spokes, which is much greater than 1, indicating that the structure is safe under the radial load condition.

4.3. Bending Load Analysis

4.3.1. Loads and Boundary Conditions

According to GB/T 5334-2021: Performance Requirements and Test Methods for Bending and Radial Fatigue of Passenger Car Wheels, the principle of the wheel bending load test is illustrated in Figure 10. In this test, the bending load applied to the wheel hub is essentially a bending moment acting at the central bore. To simulate the effect of the bending moment during the experiment, a loading arm of appropriate length is employed, so that the action of the moment is equivalently represented by an eccentric force applied at the end of the loading arm.

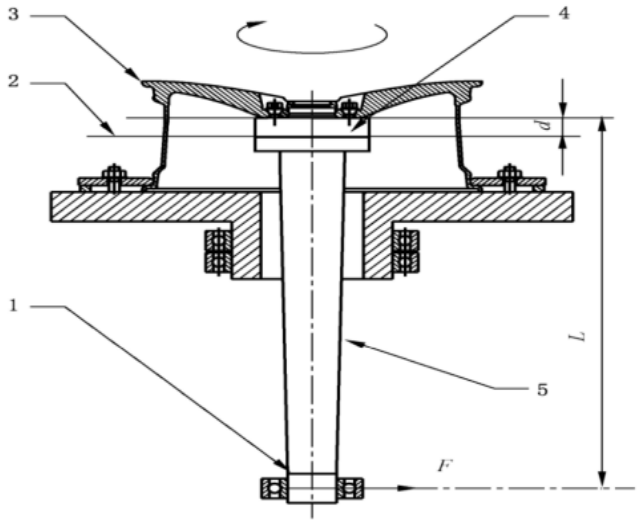

Figure 10. Principle of Bending Fatigue Test

According to GB/T 5334-2021, the magnitude of the bending moment can be expressed as:

$$M = (R \times \mu + d) \cdot F_v \cdot S \tag{3}$$

Were,

R——The tire static loaded radius is the maximum static radius of the wheel under load as specified by the vehicle or wheel manufacturer, in meters (m), $R = \frac{18\times25.4+2\times235\times0.6}{2} \times 0.001$=0.37.

μ——The tire–road surface friction coefficient was set to 0.7 (see Table 5).

d——The wheel offset, either positive or negative, was taken as 45 mm.

F_v——The maximum vertical static load or the rated load of the wheel, as specified by the vehicle or wheel manufacturer, expressed in Newtons (N).

S——The strengthening factor was set to 1.6, as listed in Table 6.

Table 6. Bending Load-Related Coefficient

Material	Coefficient of Frictionμ	Strengthening Factor$S$	Minimum Number of Cycles
Steel	0.7	1.60	30000
Aluminum Alloy	0.7	1.60	120000

Based on the aforementioned parameters, the magnitude of the bending moment MMM acting on the wheel hub was determined as $3960N \cdot m$. And the length of the loading arm was set to 400mm. Thus, the resulting eccentric force is $f = \frac{M}{L} = 9900N$, which applied at the end of the loading arm.

Fixed support constraints were imposed on the inner surface of the wheel rim to restrain hub rotation and to simulate the reactive forces from the tire. The complete loading and boundary conditions are shown in Figure 11:

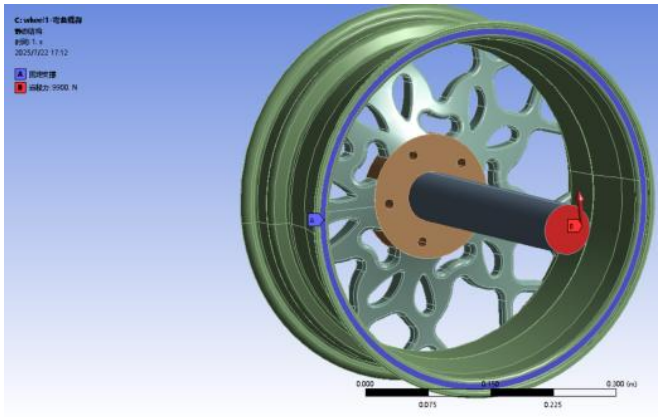

Figure 11. Diagram of Constraints and Loads for Bending Fatigue Analysis

4.3.2. Results of Bending Fatigue Analysis

A finite element simulation was conducted to analyze the bending fatigue test of the wheel hub. The results include the equivalent stress contour, total deformation contour, fatigue life contour, and safety factor contour of the wheel hub, as shown in Figures 12–14.

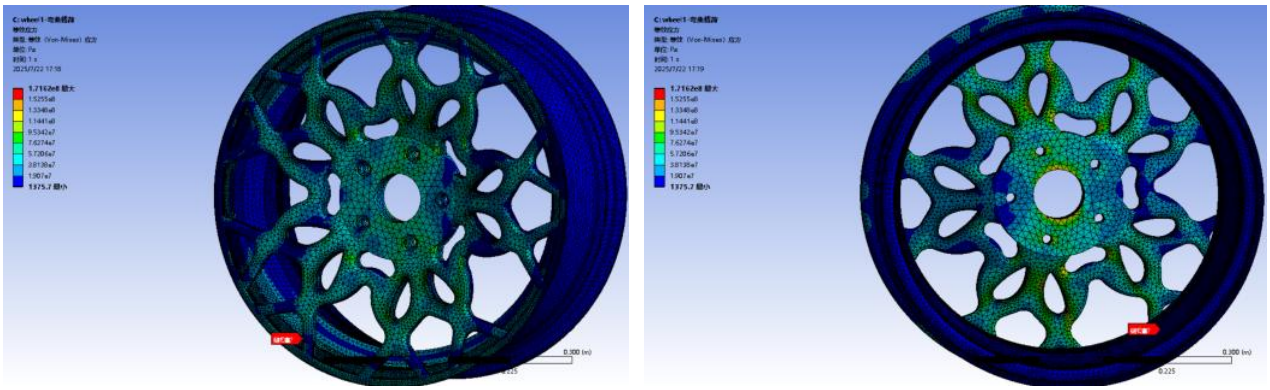

(a) Equivalent Stress Contour (Front View) (b) Equivalent Stress Contour (Rear View)

Figure 12. Equivalent Stress Contour Plot of Bending Fatigue Analysis

Figure 12 shows the equivalent stress contour under bending fatigue analysis. The ANSYS simulation indicates that the maximum equivalent stress under bending load is approximately 171 MPa, which is below the yield strength of the aluminum alloy and thus meets the design requirements. The peak stress occurs at the junction between the rim and the spokes on the rear surface, where the stress concentration is relatively high, representing a potential critical region.

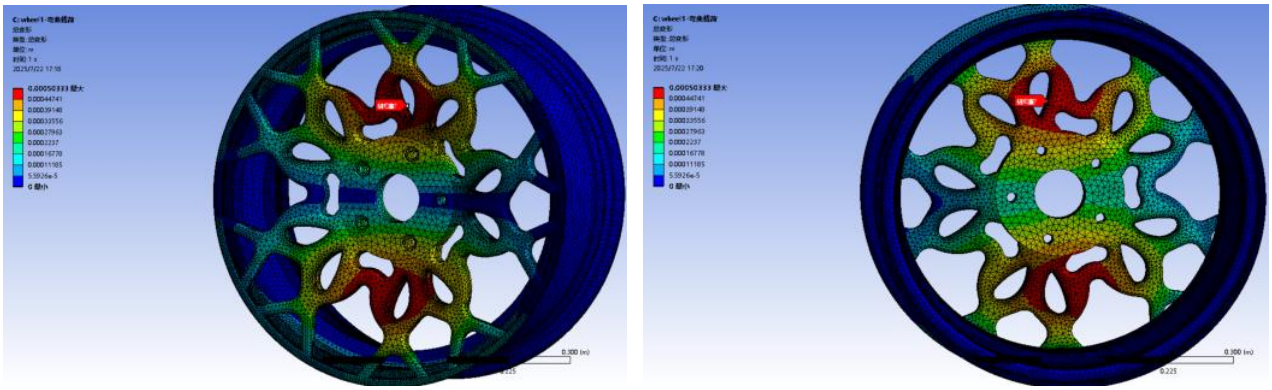

(a) Total Deformation Contour (Front View) (b) Total Deformation Contour (Rear View)

Figure 13. Total Deformation Contour Plot of Bending Fatigue Analysis

Figure 13 shows the total deformation contour under bending fatigue analysis. The ANSYS simulation indicates that the maximum deformation under bending load is approximately 0.5 mm. The maximum displacement occurs at the junction between the central claw-shaped structure and the petal-shaped structure of the spoke. The deformation is moderate and meets the design requirements.

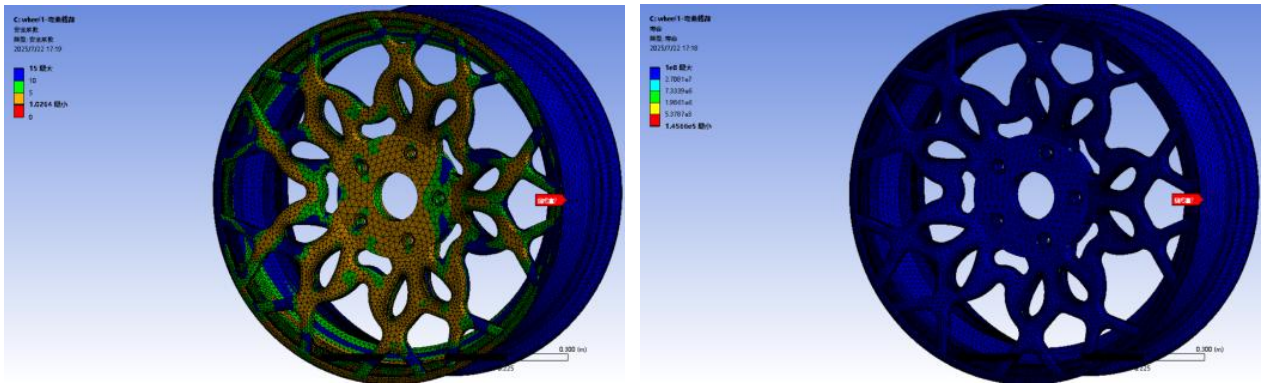

(a) Fatigue Life Contour (b) Safety Factor Contour

Figure 14. Bending fatigue analysis contour plot

Figure 14 presents the fatigue life contour under bending fatigue analysis. The S–N curve was set consistently with the radial fatigue analysis, and the minimum number of cycles was specified as 120,000 (see Table 6). The ANSYS results show that the minimum fatigue life of the wheel hub under bending load is approximately 145,000 cycles, and the minimum safety factor is about 1.03. Both occur at the junction between the rim and the spokes. Although the fatigue performance at this location meets the design requirements, the safety margin is relatively low, indicating a critical region that should be carefully monitored during actual production.

4.4. Modal Analysis

4.4.1. Theoretical Background

Modal analysis can be classified into free and constrained modes. Free modes refer to the natural vibration patterns of a structure without any constraints, while constrained modes occur under specific boundary conditions. Fundamentally, modal analysis involves a transformation and computation of coordinates. A conventional coordinate system is first established based on the actual configuration of the component, and then, through algorithmic transformation, the vectors are converted into the corresponding modal coordinates [13]. To investigate whether the wheel hub may resonate with external excitations, a free modal frequency analysis of the hub was conducted in this study.

4.4.2. Analysis Results

The wheel hub model was imported into ANSYS, with the meshing and material property settings kept consistent with those used in the static and fatigue load analyses. Since the first six frequencies in a free-free modal analysis are rigid body modes approaching zero and hold no practical significance, only the 7th to 12th modal frequencies were analyzed.

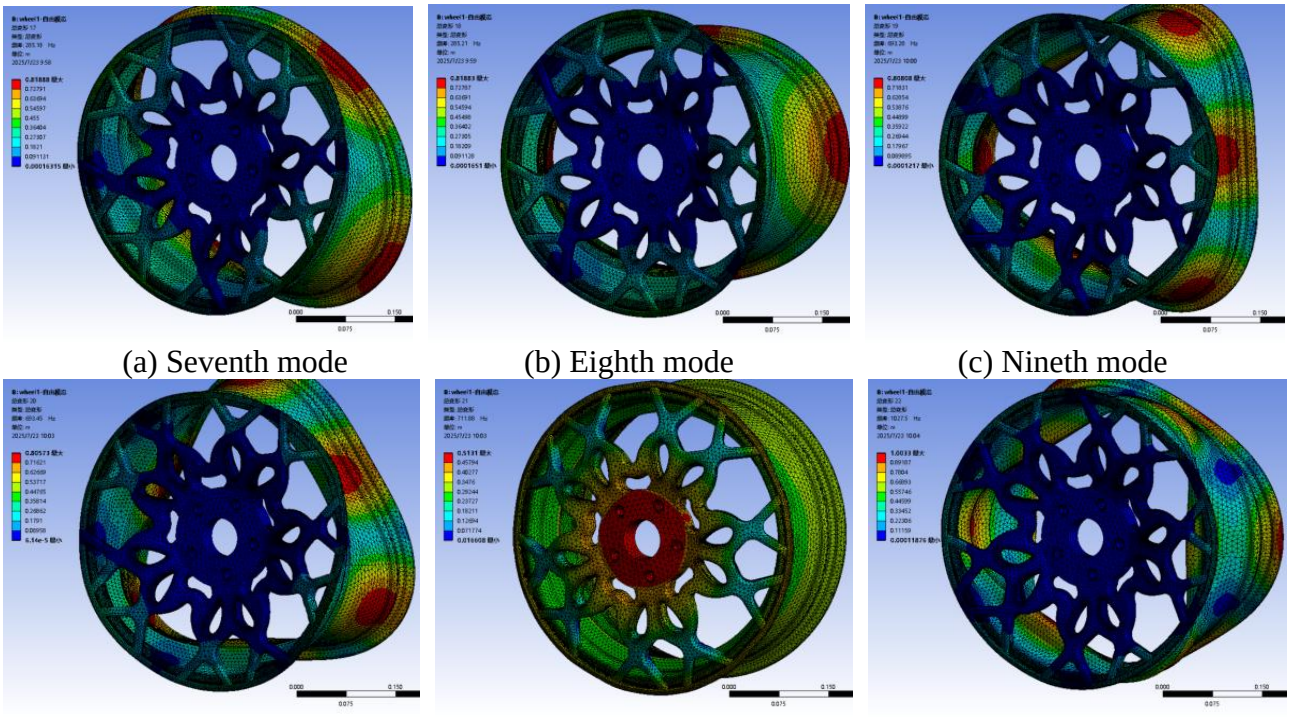

(a) Seventh mode (b) Eighth mode (c) Nineth mode

(d) Tenth mode (e) Eleventh mode (f)Twelfth mode

Figure 15. 7th to 12th mode shapes

Table 7 Frequency values of the 7th to 12th modes

7th	8th	9th	10th	11th	12th
285.18	285.21	693.28	693.45	711.88	1027.5

Figure 15 shows the mode shapes of the wheel hub from the 7th to 12th orders, while Table 7 summarizes their corresponding frequency values. These six frequency values are compared and analyzed against the possible external excitation frequencies to determine if the wheel hub will experience resonance with external stimuli.

Road surfaces are not perfectly smooth; instead, they have many small irregularities. Therefore, the excitation caused by road unevenness is one of the most common external excitations. The frequency value of road unevenness excitation is expressed as follows [14]:

$$f_{road} = un \tag{4}$$

Were,

n is spatial frequency, with a value range of $0.011m^{-1} < n < 2.83m^{-1}$;

u is vehicle speed, with a maximum speed generally not exceeding 120km/h.

Therefore, the maximum excitation frequency is calculated to be 94 Hz, which is far less than the 7th-order modal frequency, so resonance will not occur.

Driveshaft unbalance can also cause abnormal vibrations in the entire vehicle, and its excitation frequency is expressed as follows [15]:

$$f = \frac{vi_0}{2\pi r} \tag{5}$$

Were,

v represents the vehicle speed, with a maximum value of 120 km/h.

i_0 denotes the main reduction ratio, with a value of 6.1.

The vibration frequency caused by the driveshaft imbalance is 83 Hz, far below the 7th-order modal frequency, indicating that resonance will not occur.

During vehicle operation, resonance may occur when the excitation frequency induced by tire imbalance approaches the natural frequency of a certain vehicle component, which can lead to abnormal vibrations. The excitation frequency caused by tire imbalance can be expressed as follows [15]:

$$f = \frac{v}{2\pi r} \tag{6}$$

Were,

v represents the vehicle speed, with a maximum value of 120 km/h.

The excitation frequency induced by tire imbalance is calculated to be 14.7 Hz, which is much lower than the 7th-order modal frequency, indicating that resonance will not occur.

During operation, the drive motor also generates vibrations, and the vibration frequency of the drive motor can be expressed as follows:

$$f = \frac{n \times p}{60} \tag{7}$$

Were,

n denotes the rotational speed of the drive motor, with the rated speed taken as 6000 rpm.

p represents the number of pole pairs, taken as 2.

The calculated maximum driving motor frequency is 200 Hz, which is lower than the 7th-order modal frequency, indicating that resonance will not occur.

5. Conclusion

In this study, an innovative wheel hub was designed using claw-shaped and petal-shaped elements. After completing the wheel hub modeling in Creo Parametric, radial load, bending load, and modal analyses were performed using ANSYS Workbench.

(1) The radial load analysis results indicate that the maximum equivalent stress is approximately 30 MPa, well below the material yield strength, and the minimum safety factor is about 4.2. All radial fatigue test attributes of the wheel hub meet the design standards.

(2) The bending load analysis results show that the maximum equivalent stress is approximately 171 MPa, below the material yield strength, and the minimum safety factor is about 1.02. All bending fatigue test attributes of the wheel hub satisfy the design requirements.

(3) The modal analysis results indicate that under the influence of four external excitations—uneven road surfaces, tire imbalance, drive motor operation, and driveshaft imbalance—no resonance occurs, demonstrating that the design requirements are satisfied.

In summary, the claw-shaped petal wheel hub designed in this study meets the performance requirements, with a mass of 8.9 kg, achieving the goal of lightweight design. Additionally, the innovative appearance of the spokes provides valuable reference for practical production.

References

[1] Wan Tong. Application of lightweight materials and research on body structure optimization for new energy vehicles [J]. *Automotive Maintenance Technician*, 2025, (14): 116 – 117. (in Chinese).

[2] Wang Hui. Analysis of the prospects for automotive material lightweighting [J]. *Contemporary Chemical Industry Research*, 2016, (11): 123 - 124. (in Chinese).

[3] Ladhad, S., Sai, Y., Ramesh, R. *et al.* Analysis of equivalent stress, topology optimization and additive manufacturing of a wheel hub using AlSi10Mg. *Int J Mech Mater Des* (2025). https://doi.org/10.1007/s10999 - 025 - 09791 - 3.

[4] Sun, Wenlong. Research on lightweight technology for applying lightweight materials to automotive wheel hubs [D]. Beijing Institute of Technology, 2016. (in Chinese).

[5] Prem J, Raghupathi P and Kalaiyarasan A 2016 Analysis of magnesium alloy wheel for four-wheeler IJRSR 7 13126 - 30.

[6] Zhou, D., Wang, Y., Li, S. *et al.* Optimization of aluminum alloy steering knuckle for automotive lightweighting and performance enhancement. *J Braz. Soc. Mech. Sci. Eng.* 47, 327 (2025).

[7] Ferran G, Barros C R M, di Pasquale E, et al. Simplified numerical simulation of forming a car wheel disk using the SIMEX explicit FEM code, and comparisons with press-shop results [J]. Journal of Materials Processing Technology, 1996, 60 (1/2/3/4): 523 - 528.

[8] Theja M S and Krishna M V 2013 Structural and fatigue analysis of two-wheeler lighter weight alloy wheel IOSR-JMCE 8 35 - 45.

[9] Adigio E M and Nangi E O 2014 Computer aided design and simulation of radial fatigue test of automobile rim using ANSYS IOSR-JMCE 11 68 - 73.

[10] Li Xun. Research on the Influence of Finite Element Meshing on the Accuracy of Modal Calculations [J]. *Rolling Stock*, 2024, 62 (04): 101 - 105+130. (in Chinese).

[11] Yi Peng. The application of aluminum alloy in the lightweight production of automobiles [J]. *Automotive Test Report*, 2023, (13): 101 - 103. (in Chinese).

[12] Tian Jinyun. Numerical Simulation of the Automotive Wheel Hub Casting Process and Fatigue Performance Evaluation [D]. Yanshan University, 2014. (in Chinese).

[13] Chen, Yiping, Wang Xu, Liu Yi, et al. Modal Analysis of a 10 kV Power Transformer Iron Core Based on ANSYS [J]. *Equipment Maintenance Technology*, 2024, (01): 59 - 61. DOI: 10.16648/j.cnki.1005 - 2917.2024.01.014. (in Chinese).

[14] Yu, Zhisheng. *Automobile Theory* (5th ed.) [M]. Beijing: China Machine Press, 2009. (in Chinese).

[15] Sun, Zhonghui, Liu Yunbo, et al. Solution to abnormal vehicle vibration caused by driveshaft and tire unbalance [J]. *Design Calculation and Research*, 2007, 6 (9): 17 – 19. (in Chinese).